INORGANIC CHEMISTRY
FRONTIERS

RESEARCH ARTICLE

View Article Online
View Journal | View Issue

Cite this: *Inorg. Chem. Front.*, 2023, **10**, 454

Promotion of methane storage capacity with metal–organic frameworks of high porosity†

Xin Zhang, [a,b] Rui-Biao Lin, [b] Zeid A. Alothman, [c] Osamah Alduhaish,[c] Taner Yildirim,[d] Wei Zhou, [d] Jian-Rong Li *[a] and Banglin Chen *[b]

Received 21st October 2022,
Accepted 24th November 2022

DOI: 10.1039/d2qi02255a

rsc.li/frontiers-inorganic

Methane storage and onboard delivery using metal–organic frameworks (MOFs) have undergone significant development and benchmark materials with promising performance have been realized. It is still quite challenging to realize simultaneously high gravimetric and volumetric working capacities. This work analyzed the state-of-the-art MOFs with a focus on the effect of pore volume and storage temperature/pressure to achieve optimized performance. The optimal MOF pore volume range increases for storage at a slightly reduced temperature (270 K) and elevated pressure (100 bar). A new benchmark of volumetric working capacity (248 cm^3 [STP] cm^{-3}) and gravimetric working capacity (0.46 g g^{-1}) was discovered with a highly porous MOF, NPF-200, at 100–5 bar and 270 K.

Introduction

Along with the fast urbanization and industrialization of the world, there is increasing environmental pressure regarding climate change, especially global warming caused by the excessive emission of carbon dioxide.[1,2] The consumption of fossil energy is a major contributor to CO_2 emissions, while completely shifting to totally clean energy technologies such as hydrogen or photovoltaic cells is not feasible at this moment. Methane with the highest hydrogen to carbon ratio emits the lowest amount of CO_2 among all fossil fuels; therefore, it is considered as a cleaner transient energy source for the next couple of decades.[3] As a gaseous energy source of low energy density, its application in transportation requires efficient onboard storage technology. Currently, this has been realized through liquefaction at 110 K or compression at ~250 bar, which requires expensive tanks or multistage compression. Methane storage using porous sorbents is a promising technology to realize methane storage at a modest pressure (<100 bar) and near ambient temperature.[4,5]

Metal–organic frameworks (MOFs)[6] as an emerging type of crystalline porous materials have shown great potential in a variety of applications such as gas storage,[7,8] separation,[9–13] catalysis,[14,15] sensing[16–18] and so on. Ultrahigh porosity and surface areas have been realized in MOFs, making them outstanding candidates for gas storage applications. Further, their well-defined structures have enabled a deeper understanding of structure–property relationships through computational approaches[19–22] as well as empirical analysis of pore features[23] to screen or predict high performance materials. Our previous studies have established empirical equations based on the pore volume of MOFs and pore occupancy (total adsorption divided by saturated adsorption) to predict methane adsorption capacity at 35 bar and 65 bar with reasonable accuracy.[7,24] Such empirical equations could provide a promising pore volume range for MOF material screening. Finely tuning the pore size, shape and surface functionalities could further promote the adsorption capacity or working capacity.[25–30]

The practical application of methane sorbents demands simultaneously high gravimetric and volumetric capacities. The DOE (department of energy, US) suggests volumetric and gravimetric storage capacities of 350 cm^3 [STP] cm^{-3} and 0.5 g [CH_4] g^{-1}, respectively.[31] Through the above-mentioned endeavours, many benchmark materials with high gravimetric capacities have been discovered. However, it is particularly challenging to promote the volumetric capacity and a high volumetric capacity is usually realized with MOFs of moderate porosity. For example, UTSA-76a[32] with a pore volume (V_p) of 1.09 cm^3 g^{-1} exhibits a record high volumetric working capacity of 197 cm^3 [STP] cm^{-3} in the range of 65–5 bar at 298 K. Although many MOFs with a higher surface area and pore volume have been developed, their volumetric working

[a]*Beijing Key Laboratory for Green Catalysis and Separation and Department of Chemical Engineering, Faculty of Environment and Life, Beijing University of Technology, Beijing 100124, P. R. China. E-mail: jrli@bjut.edu.cn*
[b]*Department of Chemistry, University of Texas at San Antonio, One UTSA Circle, San Antonio, Texas 78249-0698, USA. E-mail: banglin.chen@utsa.edu*
[c]*Chemistry Department, College of Science, King Saud University, Riyadh 11451, Saudi Arabia*
[d]*NIST Center for Neutron Research, Gaithersburg, Maryland 20899-6102, USA*
†Electronic supplementary information (ESI) available: additional figures and tables of adsorption capacity and pore properties. See DOI: https://doi.org/10.1039/d2qi02255a

capacity was lower due to the lower material density and decreased pore occupancy. In other words, the pore space has not been fully utilized for these highly porous MOFs, and the optimal pore volume is ~1.0 cm^3 g^{-1}. One strategy to promote the pore occupancy is to decrease the storage temperature to 270 K. Under this condition, the optimal pore volume for a high volumetric working capacity shifts towards a higher porosity and a new capacity record can be realized. For example, higher volumetric working capacities of 239 cm^3 [STP] cm^{-3} and 230 cm^3 [STP] cm^{-3} were realized with NU-111 (V_p = 2.09 cm^3 g^{-1}) and MOF-177 (V_p = 1.89 cm^3 g^{-1}), respectively, with a slightly reduced temperature of 270 K.[7] Besides, slightly elevating the working pressure range to 100–5 bar could further increase the working capacity, especially for MOFs of high porosity.[33]

Herein, we analysed MOFs for methane storage at 100–5 bar and evaluated the effect of temperature on the total adsorption capacity and working capacity. Based on the relationship between adsorption capacity and pore volume, the optimal pore volume should be higher at a higher pressure and lower temperature. A new benchmark of volumetric working capacity (248 cm^3 [STP] cm^{-3}) was discovered with a highly porous MOF, NPF-200 (V_p = 2.17 cm^3 g^{-1}). This work is expected to further promote the adsorption capacity of methane through pore engineering of highly porous MOFs.

Experimental

The synthetic procedures, structural characterization and pore volume determination of NPF-200 using single crystal X-ray diffraction, PXRD, and N_2 adsorption at 77 K have been reported in our previous works.[23,34] Specifically, 12 mg (0.0133 mmol) of the tetracarboxylic ligand 4,4′,4″,4‴-((methanetetrayltetrakis(benzene-4,1-diyl))tetrakis(ethyne-2,1-diyl))tetrabenzoic acid, 14 mg (0.06 mmol) of $ZrCl_4$ and 250 mg (2.05 mmol) of benzoic acid were mixed in 2.2 mL of DMF in a 4 mL glass vial and ultrasonically dissolved. The clear solution was heated in an oven at 120 °C for 48 h. After cooling down to room temperature, colourless truncated octahedral shaped single crystals formed on the bottom and wall of the vial (yield: ~11 mg, 73%). High-pressure methane sorption measurements were performed using computer-controlled Sieverts apparatus, details of which can be found in a previous publication.[35] The gravimetric working capacity was calculated as the difference in adsorption amount at 100 bar and 5 bar from the adsorption isotherms. The gravimetric working capacity was multiplied by the crystal density in order to calculate the corresponding volumetric working capacity. The crystal density of NPF-200 was 0.389 g cm^{-3}.

Results and discussion

We first investigated the correlation between pore volume and methane total adsorption capacity at 100 bar. As shown in Fig. 1a, the gravimetric total adsorption increases as pore volume increases at both 298 and 273 K. The DOE gravimetric target can be realized by NU-1501-Fe[33] (0.52 g g^{-1}) and NU-1501-Al[33] (0.54 g g^{-1}) with a high pore volume (~2.9 cm^3 g^{-1}) at 298 K. When the storage temperature decreased to near freezing temperature (270 K), the adsorption capacity further increased. Unlike the monotonic increase of gravimetric adsorption capacity with pore volume, volumetric total adsorption capacity slightly decreases as pore volume increases (Fig. 1b), which can be attributed to the combined effect of increased gravimetric adsorption and decreased crystal density (Fig. S1†). Similar to the gravimetric adsorption, a decreased storage temperature also leads to a higher volumetric adsorption capacity. The capacity increase is more dramatic for MOFs of high pore volume, as shown in Fig. 1c; the adsorption increase percentage of mesoporous NU-1501-Al (22.2%) is much higher than that of microporous Ni-MOF-74[36] (5.9%). Such results indicate that MOFs of higher porosity and lower methane packing density (Fig. 1d) have greater potential to further promote the adsorption capacity through temperature alleviation. Correspondingly, the methane packing density also increased at 270 K, as shown in Fig. 1d.

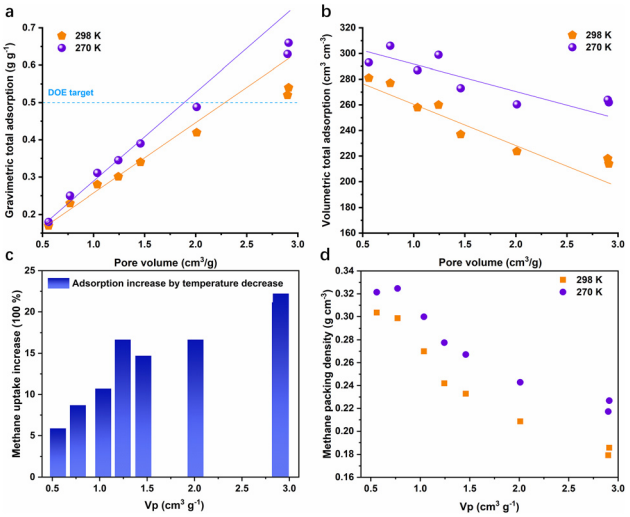

Fig. 1 Methane total adsorption at 100 bar. (a) Gravimetric adsorption at 270 K and 298 K. (b) Volumetric adsorption at 270 K and 298 K. (c) Methane uptake increase percentage upon decreasing temperature. (d) Methane packing density of MOFs with different pore volumes at 100 bar.

For onboard methane delivery, a working capacity between 100 and 5 bar is more relevant to practical usage, as 5 bar is the minimum pressure that can be utilized in a combustion engine. Therefore, we further compared the gravimetric and volumetric working capacities of different MOFs at 298 K and 273 K. As shown in Fig. 2a, the gravimetric working capacity increases as pore volume increases, which is similar to the trend of total adsorption capacity. Although a lower temperature did not always promote the working capacity, the total adsorption capacity always increased at a lower temperature.

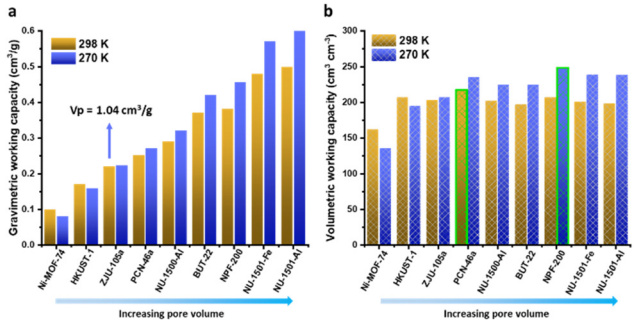

Fig. 2 Comparison of gravimetric (a) and volumetric (b) working capacities (100–5 bar) of different MOFs at 273 K and 298 K.

For MOFs of small pore volume, such as Ni-MOF-74 (0.56 cm^3 g^{-1}) and HKUST-1[36] (0.77 cm^3 g^{-1}), the working capacity decreased at 270 K. Significant working capacity promotion was realized by MOFs of high pore volume; for example, the working capacity of NU-1501-Al increased by 20%, from 0.5 g g^{-1} to 0.6 g g^{-1}. Similarly, the volumetric working capacity also increased significantly for MOFs of high porosity (Fig. 2b). The highest volumetric working capacities at 298 K and 270 K were 220 and 251 cm^3 cm^{-3}, respectively, realized by MFU-4l-Li[26] with a pore volume of 1.66 cm^3 g^{-1}. Such high working capacities are significantly higher than the benchmarks at 298 K and 65–5 bar; for example, UTSA-76a with a pore volume of 1.09 cm^3 g^{-1} exhibits a volumetric working capacity of 197 cm^3 cm^{-3}. These results indicate that a slightly lower temperature and higher pressure not only shift the optimal pore volume to a higher value, but also significantly promote the volumetric working capacity. Therefore, it is promising to develop new benchmark materials through further evaluation of MOFs with high pore volumes, and such potential has not been fully explored.

Based on the above analysis, we evaluated a highly porous Zr-MOF, NPF-200 (V_p = 2.17 cm^3 g^{-1}, S_{BET} = 5830 m^2 g^{-1}), with diverse cage types (Fig. 3a) for methane storage. NPF-200 (NPF stands for Nebraska Porous Framework) is constructed by a tetrahedral organic linker and two types of Zr clusters, exhibiting a 4,12,12 T1 topology as reported in our previous work.[34] PXRD and N_2 adsorption at 77 K (Fig. S2 and 3†) were measured to confirm the phase purity and porosity of the material before the high-pressure methane adsorption measurement. As shown in Fig. 3b, NPF-200 adsorbed a significant amount of methane at ambient and near freezing temperatures. The total adsorption capacities were 0.42 g g^{-1} and 0.51 g g^{-1} at 296 K and 270 K, respectively. Such adsorption capacities are higher than those of MFU-4l-Li (Table S1†), due to the higher pore volume of NPF-200. The gravimetric working capacities in the range of 100–5 bar were 0.38 g g^{-1} and 0.46 g g^{-1}, at 296 K and 270 K, respectively. The volumetric working capacities in the range of 100–5 bar were 207 cm^3 cm^{-3} and 248 cm^3 cm^{-3}, at 296 K and 270 K respectively. The volumetric working capacity at 270 K is higher than those of NU-1501-Fe[33] (239 cm^3 cm^{-3}) and NU-1501-Al[33] (238 cm^3 cm^{-3}), and close to the current record of MFU-4l-Li[26] (251 cm^3 cm^{-3}). Meanwhile, the gravimetric working capacity of NPF-200 at 270 K (0.46 g g^{-1}) is higher than that of MFU-4l-Li (0.38 g g^{-1}). Therefore, NPF-200 represents a new benchmark material with simultaneously high gravimetric and volumetric working capacities, as shown in Fig. 3c. The adsorption performance of NPF-200 fits well with the above-discussed general correlation, and indicates that the optimal pore volume is likely ~2.0 cm^3 g^{-1} (between those of NPF-200 and MFU-4l-Li). Such an optimal pore volume is also much higher than that of benchmark materials for storage at 298 K and 65 bar and demonstrates the potential of MOFs with higher pore volumes.

Besides the effect of pore volume, the pore structure also contributes significantly to the storage capacity. Compared to BUT-22[37] with a similar pore volume (2.01 cm^3 g^{-1}), the NPF-200 material exhibits the same gravimetric total adsorption (0.42 g g^{-1}) and a higher working capacity (Table S1†). Such a result indicates a lower adsorption at 5 bar for NPF-200. At 270 K, NPF-200 exhibits superior performance to BUT-22, with a working capacity of 0.46 g g^{-1} *vs.* 0.42 g g^{-1} of

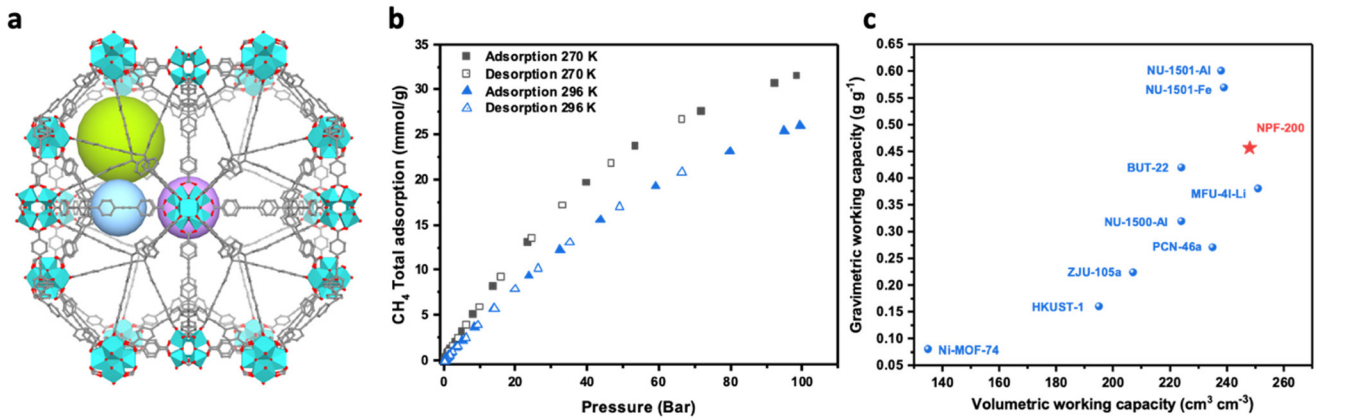

Fig. 3 (a) Structure of NPF-200 with spheres representing different cages. (b) Methane adsorption isotherm of NPF-200 measured at 270 K and 298 K. (c) Comparison of gravimetric *vs.* volumetric working capacities of reported MOFs in the 100–5 bar pressure range.

BUT-22. The superior working capacity of NPF-200 may be attributed to its lower adsorption at 5 bar, due to the lack of ultra-micropores (pore size of 1.5–2.5 nm, as shown in Fig. S4†) and open metal sites. In addition, the cage-type pore geometry may also contribute to the high adsorption capacity, as revealed by previous works.[23,38,39] The heat of adsorption (Q_{st}) was calculated using the Virial method and Clausius–Clapeyron equation with adsorption isotherms recorded at 270 K and 296 K, as shown in Fig. S5.† Both methods provide a similar Q_{st} value of 10.7 kJ mol^{-1}, which is smaller than those of BUT-22[37] (12 kJ mol^{-1}), HKUST-1[36] (17 kJ mol^{-1}), MOF-5[36] (12.3 kJ mol^{-1}).

Conclusions

In summary, we have analysed the general correlation between methane adsorption capacity at 100 bar and pore volume. The gravimetric total adsorption capacity and working capacity increase monotonically with pore volume. The volumetric total adsorption slightly decreases for MOFs of high pore volume, due to their lower crystal density. Decreased temperature (from 296 K to 270 K) significantly promoted the volumetric working capacity of the MOFs with higher pore volume. Further, a new benchmark material with simultaneously high gravimetric and volumetric working capacities was achieved with a highly porous MOF, NPF-200 (pore volume of 2.17 cm^3 g^{-1}). By comparing MOFs applied in storage at 65–5 bar and 298 K, the results indicate that a higher pore volume of ~2.0 cm^3 g^{-1} might be optimal for storage at 100–5 bar and 270 K. This work is expected to further promote the methane volumetric working capacity at 100 bar through pore engineering of highly porous MOFs.

Author contributions

Xin Zhang: data curation, formal analysis, investigation, writing – original draft; Rui-Biao Lin: formal analysis; Zeid A. Alothman: formal analysis, funding acquisition; Osamah Alduhaish: formal analysis, funding acquisition; Taner Yildirim: isotherm data collection and analysis; Wei Zhou: isotherm data collection and analysis; Jian-Rong Li: supervision, writing – review & editing; Banglin Chen: conceptualization, supervision, writing – review & editing, funding acquisition.

Conflicts of interest

There are no conflicts to declare.

Acknowledgements

The authors extend their appreciation to the Deputyship for Research & Innovation, Ministry of Education, in Saudi Arabia for funding this research work through Project number (DRI-KSU-572). X. Zhang acknowledges the financial support from the National Natural Science Foundation of China (No. 22108007).

References

1 S. Solaymani, CO_2 emissions patterns in 7 top carbon emitter economies: The case of transport sector, *Energy*, 2019, **168**, 989–1001.
2 Z. Liu, Z. Deng, G. He, H. L. Wang, X. Zhang, J. Lin, Y. Qi and X. Liang, Challenges and opportunities for carbon neutrality in China, *Nat. Rev. Earth Environ.*, 2022, **3**, 141–155.
3 D. Saha, H. A. Grappe, A. Chakraborty and G. Orkoulas, Postextraction Separation, On-Board Storage, and Catalytic Conversion of Methane in Natural Gas: A Review, *Chem. Rev.*, 2016, **116**, 11436–11499.
4 T. A. Makal, J.-R. Li, W. Lu and H.-C. Zhou, Methane storage in advanced porous materials, *Chem. Soc. Rev.*, 2012, **41**, 7761–7779.
5 V. C. Menon and S. Komarneni, Porous Adsorbents for Vehicular Natural Gas Storage: A Review, *J. Porous Mater.*, 1998, **5**, 43–58.
6 H. Furukawa, K. E. Cordova, M. O'Keeffe and O. M. Yaghi, The chemistry and applications of metal-organic frameworks, *Science*, 2013, **341**, 1230444.
7 B. Li, H.-M. Wen, W. Zhou, J. Q. Xu and B. Chen, Porous Metal-Organic Frameworks: Promising Materials for Methane Storage, *Chem*, 2016, **1**, 557–580.
8 J. A. Mason, J. Oktawiec, M. K. Taylor, M. R. Hudson, J. Rodriguez, J. E. Bachman, M. I. Gonzalez, A. Cervellino, A. Guagliardi, C. M. Brown, P. L. Llewellyn, N. Masciocchi and J. R. Long, Methane storage in flexible metal-organic frameworks with intrinsic thermal management, *Nature*, 2015, **527**, 357–361.
9 J.-B. Lin, T. T. T. Nguyen, R. Vaidhyanathan, J. Burner, J. M. Taylor, H. Durekova, F. Akhtar, R. K. Mah, O. Ghaffari-Nik, S. Marx, N. Fylstra, S. S. Iremonger, K. W. Dawson, P. Sarkar, P. Hovington, A. Rajendran, T. K. Woo and G. K. H. Shimizu, A scalable metal-organic framework as a durable physisorbent for carbon dioxide capture, *Science*, 2021, **374**, 1464–1469.
10 T. He, X.-J. Kong, Z.-X. Bian, Y.-Z. Zhang, G.-R. Si, L.-H. Xie, X.-Q. Wu, H. Huang, Z. Chang, X.-H. Bu, M. J. Zaworotko, Z. R. Nie and J.-R. Li, Trace removal of benzene vapour using double-walled metal-dipyrazolate frameworks, *Nat. Mater.*, 2022, **21**, 689–695.
11 O. T. Qazvini, R. Babarao, Z. L. Shi, Y. B. Zhang and S. G. Telfer, A Robust Ethane-Trapping Metal-Organic Framework with a High Capacity for Ethylene Purification, *J. Am. Chem. Soc.*, 2019, **141**, 5014–5020.
12 Z. Jiang, L. Fan, P. Zhou, T. Xu, S. Hu, J. Chen, D.-L. Chen and Y. He, An aromatic-rich cage-based MOF with inorganic chloride ions decorating the pore surface displaying the preferential adsorption of C_2H_2 and C_2H_6 over C_2H_4, *Inorg. Chem. Front.*, 2021, **8**, 1243–1252.

13 K. Shao, H. M. Wen, C. C. Liang, X. Xiao, X. W. Gu, B. Chen, G. Qian and B. Li, Engineering Supramolecular Binding Sites in a Chemically Stable Metal-Organic Framework for Simultaneous High C_2H_2 Storage and Separation, *Angew. Chem., Int. Ed.*, 2022, **61**, e202211523.
14 N. Li, J. Liu, J.-J. Liu, L.-Z. Dong, Z.-F. Xin, Y.-L. Teng and Y.-Q. Lan, Adenine Components in Biomimetic Metal-Organic Frameworks for Efficient CO_2 Photoconversion, *Angew. Chem., Int. Ed.*, 2019, **58**, 5226–5231.
15 Y. Tang, L. Zhao, G. F. Ji, Y. Zhang, C. He, Y.-F. Wang, J.-W. Wei and C.-Y. Duan, Ligand-regulated metal-organic frameworks for synergistic photoredox and nickel catalysis, *Inorg. Chem. Front.*, 2022, **9**, 3116–3129.
16 Y. Cui, J. Zhang, H. He and G. Qian, Photonic functional metal-organic frameworks, *Chem. Soc. Rev.*, 2018, **47**, 5740–5785.
17 B. Wang, X.-L. Lv, D. Feng, L. H. Xie, J. Zhang, M. Li, Y. Xie, J.-R. Li and H.-C. Zhou, Highly Stable Zr(IV)-Based Metal-Organic Frameworks for the Detection and Removal of Antibiotics and Organic Explosives in Water, *J. Am. Chem. Soc.*, 2016, **138**, 6204–6216.
18 S. A. Diamantis, A. Margariti, A. D. Pournara, G. S. Papaefstathiou, M. J. Manos and T. Lazarides, Luminescent metal–organic frameworks as chemical sensors: common pitfalls and proposed best practices, *Inorg. Chem. Front.*, 2018, **5**, 1493–1511.
19 S. Y. Kim, S. Han, S. Lee, J. H. Kang, S. Yoon, W. Park, M. W. Shin, J. Kim, Y. G. Chung and Y. S. Bae, Discovery of High-Performing Metal-Organic Frameworks for On-Board Methane Storage and Delivery via LNG-ANG Coupling: High-Throughput Screening, Machine Learning, and Experimental Validation, *Adv. Sci.*, 2022, **9**, 2201559.
20 K. Nath, A. Ahmed, D. J. Siegel and A. J. Matzger, Computational Identification and Experimental Demonstration of High-Performance Methane Sorbents, *Angew. Chem., Int. Ed.*, 2022, **61**, e202203575.
21 D. A. Gómez-Gualdrón, Y. J. Colón, X. Zhang, T. C. Wang, Y.-S. Chen, J. T. Hupp, T. Yildirim, O. K. Farha, J. Zhang and R. Q. Snurr, Evaluating topologically diverse metal–organic frameworks for cryo-adsorbed hydrogen storage, *Energy Environ. Sci.*, 2016, **9**, 3279–3289.
22 M. Suyetin, The application of machine learning for predicting the methane uptake and working capacity of MOFs, *Faraday Discuss.*, 2021, **231**, 224–234.
23 X. Zhang, R.-B. Lin, J. Wang, B. Wang, B. Liang, T. Yildirim, J. Zhang, W. Zhou and B. Chen, Optimization of the Pore Structures of MOFs for Record High Hydrogen Volumetric Working Capacity, *Adv. Mater.*, 2020, **32**, e1907995.
24 Y. He, W. Zhou, T. Yildirim and B. Chen, A series of metal–organic frameworks with high methane uptake and an empirical equation for predicting methane storage capacity, *Energy Environ. Sci.*, 2013, **6**, 2735–2744.
25 D. Alezi, I. Spanopoulos, C. Tsangarakis, A. Shkurenko, K. Adil, Y. Belmabkhout, M. Eddaoudi and P. N. Trikalitis, Reticular Chemistry at Its Best: Directed Assembly of Hexagonal Building Units into the Awaited Metal-Organic Framework with the Intricate Polybenzene Topology, pbz-MOF, *J. Am. Chem. Soc.*, 2016, **138**, 12767–12770.
26 Z. Chen, M. R. Mian, S. J. Lee, H. Chen, X. Zhang, K. O. Kirlikovali, S. Shulda, P. Melix, A. S. Rosen, P. A. Parilla, T. Gennett, R. Q. Snurr, T. Islamoglu, T. Yildirim and O. K. Farha, Fine-Tuning a Robust Metal-Organic Framework toward Enhanced Clean Energy Gas Storage, *J. Am. Chem. Soc.*, 2021, **143**, 18838–18843.
27 Y. Peng, V. Krungleviciute, I. Eryazici, J. T. Hupp, O. K. Farha and T. Yildirim, Methane storage in metal-organic frameworks: current records, surprise findings, and challenges, *J. Am. Chem. Soc.*, 2013, **135**, 11887–11894.
28 I. Spanopoulos, C. Tsangarakis, E. Klontzas, E. Tylianakis, G. Froudakis, K. Adil, Y. Belmabkhout, M. Eddaoudi and P. N. Trikalitis, Reticular Synthesis of HKUST-like tbo-MOFs with Enhanced CH_4 Storage, *J. Am. Chem. Soc.*, 2016, **138**, 1568–1574.
29 B. Li, H.-M. Wen, H. Wang, H. Wu, T. Yildirim, W. Zhou and B. Chen, Porous metal–organic frameworks with Lewis basic nitrogen sites for high-capacity methane storage, *Energy Environ. Sci.*, 2015, **8**, 2504–2511.
30 G. Verma, S. Kumar, H. Vardhan, J. Ren, Z. Niu, T. Pham, L. Wojtas, S. Butikofer, J. C. Echeverria Garcia, Y.-S. Chen, B. Space and S. Ma, A robust soc-MOF platform exhibiting high gravimetric uptake and volumetric deliverable capacity for on-board methane storage, *Nano Res.*, 2020, **14**, 512–517.
31 See the DOE MOVE program at, **https://arpa-e.energy.gov/?q=arpa-e-programs/move**.
32 B. Li, H. M. Wen, H. Wang, H. Wu, M. Tyagi, T. Yildirim, W. Zhou and B. Chen, A porous metal-organic framework with dynamic pyrimidine groups exhibiting record high methane storage working capacity, *J. Am. Chem. Soc.*, 2014, **136**, 6207–6210.
33 Z. Chen, P. Li, R. Anderson, X. Wang, X. Zhang, L. Robison, L. R. Redfern, S. Moribe, T. Islamoglu, D. A. Gomez-Gualdron, T. Yildirim, J. F. Stoddart and O. K. Farha, Balancing volumetric and gravimetric uptake in highly porous materials for clean energy, *Science*, 2020, **368**, 297–303.
34 X. Zhang, X. Zhang, J. A. Johnson, Y.-S. Chen and J. Zhang, Highly Porous Zirconium Metal-Organic Frameworks with beta-UH_3-like Topology Based on Elongated Tetrahedral Linkers, *J. Am. Chem. Soc.*, 2016, **138**, 8380–8383.
35 W. Zhou, H. Wu, M. R. Hartman and T. Yildirim, Hydrogen and Methane Adsorption in Metal–Organic Frameworks: A High-Pressure Volumetric Study, *J. Phys. Chem. C*, 2007, **111**, 16131–16137.
36 J. A. Mason, M. Veenstra and J. R. Long, Evaluating metal–organic frameworks for natural gas storage, *Chem. Sci.*, 2014, **5**, 32–51.
37 B. Wang, X. Zhang, H. Huang, Z. Zhang, T. Yildirim, W. Zhou, S. Xiang and B. Chen, A microporous aluminum-based metal-organic framework for high methane, hydrogen, and carbon dioxide storage, *Nano Res.*, 2020, **14**, 507–511.

38 J. Pei, H. M. Wen, X. W. Gu, Q. L. Qian, Y. Yang, Y. Cui, B. Li, B. Chen and G. Qian, Dense Packing of Acetylene in a Stable and Low-Cost Metal-Organic Framework for Efficient C_2H_2 /CO_2 Separation, *Angew. Chem., Int. Ed.*, 2021, **60**, 25068–25074.

39 C. C. Liang, Z. L. Shi, C. T. He, J. Tan, H. D. Zhou, H. L. Zhou, Y. Lee and Y. B. Zhang, Engineering of Pore Geometry for Ultrahigh Capacity Methane Storage in Mesoporous Metal-Organic Frameworks, *J. Am. Chem. Soc.*, 2017, **139**, 13300–13303.